

Algorithm for atmospheric corrections of aircraft and satellite imagery

R. S. FRASER, R. A. FERRARE†, Y. J. KAUFMAN†

Laboratory for Atmospheres, Goddard Space Flight Center, Greenbelt,
Maryland 20771, U.S.A.

B. L. MARKHAM

Laboratory for Terrestrial Physics, Goddard Space Flight Center, Greenbelt,
Maryland 20771, U.S.A.

and S. MATTOO‡

Applied Research Corporation, Landover, Maryland 20785, U.S.A.

(Received 13 April 1990)

Abstract. An algorithm is described for making fast atmospheric corrections. The required radiation parameters are stored in a lookup table. The procedure is to enter the lookup table with the measured radiance, wavelength, view and illumination directions, heights of observation and surface, and the aerosol and gaseous absorption optical thicknesses. The surface radiance, the irradiance incident on a surface, and surface reflectance are computed then. Alternately, the program will compute the upward radiances at specific altitudes for a given surface reflectance, view and illumination directions, and aerosol and gaseous absorption optical thicknesses.

1. Introduction

1.1 Background

This paper describes a fast and simple atmospheric correction algorithm to derive the surface reflectance, surface radiance, and incident irradiance from radiances measured by satellite or aircraft in the visible and near-infrared parts of the spectrum. The original version of this algorithm was developed to correct the radiances measured during FIFE (First ISLSCP Field Experiment) (Sellers *et al.* 1988), which has taken place at the Konza Prairie in Kansas. While the algorithm has been designed to correct radiances measured over a rural site for the wavelength range $0.48 \mu\text{m} \leq \lambda \leq 2.2 \mu\text{m}$, a sensitivity study has shown that the algorithm can be a practical tool for many applications of remote sensing, for which a uniform surface can be assumed, and for which the optical characteristics of the aerosol do not differ significantly from the rural aerosol (the algorithm should not be applied for correcting for the effect of desert dust or fog). In essence, the algorithm simplifies the

†Laboratory for Atmospheres and Universities Space Research Association Resident Associate.

‡This work was done under contract at the Goddard Space Flight Center, Greenbelt, Maryland, U.S.A.

atmospheric correction procedure to a desktop operation, by sacrificing the flexibility to select specific aerosol size distributions and refractive indexes, but not optical thickness.

1.2. *The intervening atmosphere*

The atmosphere affects satellite images of the Earth's surface in the solar spectrum in two ways. Path radiance is created by sunlight scattered towards the sensor by atmospheric molecules, aerosols, and clouds. In addition, solar energy that is reflected from the Earth's surface and serves as the remote sensing signal is attenuated by the atmosphere. This combined atmospheric effect is wavelength dependent, varies in time and space, and depends on the surface reflectance and its spatial variation. Correction for the atmospheric effect can produce remote sensing signals that are more closely related to the surface characteristics. Molecular scattering and absorption in the atmosphere are accounted for satisfactorily. Gaseous absorption is minimized by choosing sensor bands in atmospheric windows. Therefore, aerosol scattering and absorption, and the presence of subpixel clouds, are the main variables in the atmospheric effect on satellite imagery. This algorithm neglects cloud effects but accounts for all other significant atmospheric radiation effects.

1.3. *Atmospheric corrections*

The only atmospheric parameters required by the algorithm are the aerosol and gaseous optical thicknesses. The algorithm has default values for the gaseous optical thicknesses, however. The aerosol optical thickness can be obtained from three sources. Climatology supplies the least accurate value, since the data are sparse and available only for a few wavelengths. Accurate values can be obtained from ground-based values of the measurement of solar transmission. Such observations would coincide with aircraft or satellite measurements. The aerosol optical thickness can be obtained from the remote measurements themselves. Examples include deriving optical thickness of many land surfaces in the blue spectrum, dense dark vegetation in the visible spectrum (Kaufman and Sendra 1988), and water in the red and near-infrared. Kaufman *et al.* (1990) and Ferrare *et al.* (1990) have developed improved methods of estimating the aerosol optical thickness, scattering phase function, and albedo of single scattering. The accuracy of estimating the optical thickness from satellite observations over land is $\Delta\tau_a=0.1$ for the spectral bands where the measurements are made, if the aerosol optical thickness $\tau_a < 0.5$. The regions selected for estimating the optical thickness have to be exclusive of areas where surface features are being measured.

1.4. *The algorithm*

The algorithm is designed to compute the surface reflectance for a given measured radiance, or alternatively, the upward radiance at an arbitrary height when the surface reflectance is given. The algorithm is applicable to many wavelengths in the visible and near-infrared spectrum (with appropriately specified gaseous absorption), for a wide range of solar and observation zenith angles, azimuth angles between the observer and the solar rays, and any height of the observer (aircraft or satellite). Any practical value of the aerosol optical thickness can be used, but the tabulated radiation parameters are computed for a specific aerosol size distribution and refractive indices.

The relation between the measured radiance and the surface reflectance is expressed as a function of the path radiance, downward flux at the ground, atmospheric transmission, and the atmospheric backscattering ratio. Using this relation, a lookup table is constructed which relates the measured upward radiance to surface reflectance for several aerosol optical thicknesses, solar zenith angles, measurement wavelengths, and a range of observation directions. This lookup table is based on the tabulation of the results of radiative transfer computations which are made using a Dave (1972 a, b, c, d) code. It is assumed that the atmosphere and surface are horizontally homogeneous, and the surface reflects light according to Lambert's law. The light scattered by the atmosphere and the surface is assumed to be unpolarized. The atmosphere is also assumed to be cloud-free. For the most part, aerosol extinction is the dominant parameter in the aerosol component of the atmospheric effect (Fraser and Kaufman 1985). Thus, in this algorithm the aerosol optical thickness is the only variable aerosol parameter. The algorithm uses a constant aerosol single scattering phase function and scattering albedo chosen to represent a rural environment. In the following the mathematical basis of the algorithm is given. Details of applying it are discussed. Finally, an error analysis is made.

2. Mathematical description

In order to correct for the atmospheric effects, a relation is developed between the upward spectral radiance L^m measured from satellite or aircraft and the surface reflectance ρ . The radiance is equivalent to the specific intensity as defined by Chandrasekhar (1950), except that the radiance, as used here, is the radiant energy within a unit wavelength interval instead of the energy per unit frequency. The radiance L^m can be expressed explicitly as a function of the path radiance L_0 (upward radiance for zero surface reflectance), the downward flux through a horizontal surface at the ground F_d (for zero surface reflectance), the total (direct + diffuse) transmission from the surface to the observer T , and the atmospheric backscattering ratio s . It is assumed that the atmosphere and the surface are horizontally homogeneous, but the atmospheric optical properties vary in the vertical direction. The surface is assumed to reflect light according to Lambert's law. The light scattered by the cloud-free atmosphere and surface is assumed to be unpolarized. The relation between L^m and ρ is (Chandrasekhar 1950)

$$L^m = L_0 + \frac{(\rho F_d T)}{\pi(1 - s\rho)} \quad (1)$$

Here L^m is a function of λ , θ_0 , τ_a , τ_{gs} , ω_0 , τ_g , θ , Z_0 , Z , and ϕ , where λ is the wavelength of the radiation. θ_0 is the solar zenith angle. τ_a is the aerosol optical thickness (all optical thicknesses apply to the vertical direction and are used with base e). τ_{gs} is the molecular scattering optical thickness, ω_0 is the ratio of the aerosol scattering and extinction optical thicknesses, the albedo of single scattering, τ_g is the gaseous absorption optical thickness, Z is the observation height, Z_0 is the height of the surface above sea level (14), θ is the propagation direction zenith angle of the radiant energy at the ground, and ϕ is the azimuth angle (azimuthal angles are measured with respect to the principal plane through the sun; $\phi = 0^\circ$ lies in the plane containing the direction of propagation of the direct sunlight).

The functions L_0 , T , F_d and s are computed with the following functional dependences:

$$\begin{aligned} L_0 &= L_0(\lambda, \theta_0, \tau_a, \tau_{gs}, \tau_g, \omega_0, Z_0, Z, \theta, \phi) & F_d &= F_d(\lambda, \theta_0, \tau_a, \tau_{gs}, \tau_g, Z_0, \omega_0) \\ T &= T(\lambda, \tau_a, \tau_{gs}, \tau_g, \omega_0, Z_0, Z, \theta), & s &= s(\lambda, \tau_a, \tau_{gs}, \tau_g, Z_0, \omega_0) \end{aligned}$$

The correction algorithm is based on the inverse of (1), where the surface reflectance ρ can be expressed in terms of the measured radiance L^m :

$$\rho = \frac{f}{(1 + sf)} \quad (2)$$

where

$$f = \frac{\pi(L^m - L_0)}{(F_d T)} \quad (3)$$

The algorithm will compute L^m using (1) if ρ is given or will compute ρ using (2) and (3) if L^m is given. Other computed quantities are the total irradiant flux F_g on a horizontal surface at the ground,

$$F_g = \frac{F_d}{(1 - s\rho)} \quad (4)$$

and the upward radiance L_g at the ground in the direction of observation

$$L_g = \frac{\rho F_g}{\pi} \quad (5)$$

3. Algorithm

3.1. Model wavelengths

The lookup is computed for the following wavelengths: 0.639, 0.845, 0.486, 0.587, 0.663, 0.837, 1.663, and 2.189 μm , which were chosen to represent the NOAA-9 AVHRR band 1 (0.58–0.68 μm), band 2 (0.725–1.10 μm); the Landsat-5 TM band 1 (0.45–0.52 μm), band 2 (0.52–0.60 μm), band 3 (0.63–0.69 μm), band 4 (0.76–0.90 μm), band 5 (1.55–1.80 μm), and band 7 (2.10–2.35 μm). These wavelengths are listed in table 1. They are suitable for correcting measurements from instruments with essentially the same spectral responses. These instruments are the NOAA 7-11 AVHRR, the Landsat TM 4, and the TM simulator (NS004).

The wavelengths chosen to represent a particular band is computed by first calculating λ^*

$$\lambda^* = \frac{\int \lambda L^m F_0 \psi d\lambda}{\int L^m F_0 \psi d\lambda} \quad (6)$$

where L^m = normalized radiance at the top of the atmosphere, F_0 = extraterrestrial solar spectral flux, and ψ = response function of the sensor. The values for F_0 are obtained from Neckel and Labs (1984) while the values for ψ correspond to the specific sensor. For the NOAA-9 AVHRR and Landsat TM sensors, these values are obtained from Kidwell (1985) and Markham and Barker (1985), respectively. The effective wavelength λ^* in (6) is a function of the normalized radiance, which is a function of the surface reflectance, aerosol optical thickness, and geometry. The

Table 1. Spectral bands, aerosol refractive indices, and optical thicknesses.

	AVHRR		TM					
	1	2	1	2	3	4	5	7
Sensor wavelengths								
50% minimum response (nm)	569.8	714.3	452.4	528.0	626.4	776.4	1567.4	2097.2
50% maximum response (nm)	699.3	982.2	517.8	609.3	693.2	904.5	1784.1	2349.0
Peak response (nm)	680.0	760.0	503.0	594.0	677.0	800.0	1710.0	2200.0
Model (equation 6)(nm)	639.0	844.6	486.2	586.9	662.7	837.3	1662.7	2188.6
Indices of refraction								
n' (accumulation mode)	1.43	1.43	1.43	1.43	1.43	1.43	1.40	1.40
k (accumulation mode)	10^{-8}	10^{-8}	10^{-8}	10^{-8}	10^{-8}	10^{-8}	10^{-4}	10^{-4}
n' (coarse particle mode)	1.53	1.53	1.53	1.53	1.53	1.53	1.40	1.35
k (coarse particle mode)	10^{-7}	10^{-7}	10^{-7}	10^{-7}	10^{-7}	10^{-7}	10^{-4}	0.00814
Optical thicknesses								
Molecular scattering τ_{rs}	0.0540	0.0180	0.159	0.0841	0.0449	0.0176	0.0012	0.0004
Gaseous absorption								
ozone $\tau_{r O_3}$	0.0240	0.00064	0.00663	0.0317	0.0174	0.0000	0.0000	0.0000
water vapour $\tau_{r H_2O}$	0.00605	0.0933	0.0000	0.0002	0.0068	0.0410	0.0957	0.0741
carbon dioxide $\tau_{r CO_2}$	0.00071	0.0146	0.0000	0.0000	0.0000	0.0021	0.0077	0.0091
Aerosol albedo of single scattering ω_0	0.941	0.911	0.948	0.943	0.940	0.913	0.829	0.865
Composite (§3.3)								
τ_r^H	0.0247	0.0152	0.0066	0.0317	0.0174	0.00206	0.00771	0.00908
τ_r^L	0.00605	0.0933	0.0000	0.0002	0.0068	0.0410	0.0957	0.0741

Algorithm for atmospheric correction

normalized radiance is computed for a model of the earth-atmosphere system representative of surface and atmospheric conditions expected for the FIFE Konza Prairie site during the summer. A similar approach can be used to determine the wavelengths which correspond to other sensors.

The correction algorithm is based on the tabulation of the results of radiative transfer computations of L'_0 , F'_d , s , and T . The primed parameters are normalized flux and radiance rather than their absolute values. The normalized values are related to their corresponding absolute values by the following equations:

$$F'_d(\theta_0, \tau_a) = \frac{F_d}{F_0 \cos \theta_0}, \quad L'_0(\theta_0, \theta, \phi, \tau_a, Z_0, Z) = \frac{\pi L_0}{F_0 \cos \theta_0}. \quad (7)$$

In order to use the table for atmospheric correction, the measured absolute radiance L_m is converted to L_m' using

$$L_m' = \frac{\pi L_m}{F_0 \cos \theta_0} \quad (8)$$

where

$$F_0 = F_o R^2, \quad R = d/d' \quad (9)$$

d is Earth-Sun distance for the day of the year when measurements are made, and d' is the mean Earth-Sun distance.

The algorithm is generalized to accept any wavelength in the range 0.49 to 0.83 μm , 0.84, 1.66, and 2.19 μm . For wavelengths for which there are not entries in the lookup table (see table 1), the algorithm will interpolate the atmospheric functions (L'_0 , T , F'_d , s) for the desired wavelength. The interpolation is performed assuming that these parameters are proportional to the wavelength raised to a power, which is computed from the tabulated data: for example, $\log T \sim \log \lambda$. The only nonlinear relations are between the gaseous absorptions for the different wavelengths. Correction for the gaseous absorption is discussed in §3.4.

3.2. Aerosol properties

Because the absorption and scattering of light by atmospheric aerosols is highly variable, some assumptions regarding the size, shape, and composition of the aerosol must be made. In this model, the aerosols are assumed to be spheres so that Mie theory can be used to calculate the scattering by aerosols. Although in general the aerosol particles are not spherical, it is assumed that the sizes assigned to the aerosol particles are the sizes of spheres that have similar scattering properties to the measured aerosol distribution (Shettle and Fenn 1979). This assumption has further basis because it has been found that the aerosol particles become more spherical as the relative humidity increases (Nilsson 1979).

The algorithm uses a bimodal aerosol size distribution consisting of an accumulation mode ($0.1 \mu\text{m} \leq d \leq 1.0 \mu\text{m}$) and a coarse particle mode ($d > 0.5 \mu\text{m}$). Their size distribution is represented by the sum of two log-normal distributions. The number density function of particles of radius r is (Shettle and Fenn 1979)

$$n(r) = \frac{dN(r)}{dr} = \sum_{i=1}^2 \left[\frac{N_i}{\ln(10)r\sigma_{i\sqrt{e}}(2\pi)} \right] \exp \left[\frac{-(\log r - \log r_n^i)^2}{2\sigma_i^2} \right] \quad (10)$$

where $N(r)$ = cumulative number density of particles of radius r , σ_i = standard deviation of the logarithm of the radius, r_n^i = geometric mean radius, N_i = total number density in i th mode. The values of N_i , r_n^i , and σ_i used in the model correspond to the 70 per cent relative humidity, rural aerosol model of Shettle and Fenn (1979); these values are shown in table 2. The values of N_i shown in table 2 are normalized such that $N_1 + N_2 = 1$ particle/cm³. This bimodal aerosol size distribution is assumed constant with height.

The aerosol composition is expressed in terms of the complex refractive index $n = n' - ik$. The refractive index for both the accumulation and coarse particle modes depends on wavelength. Five different real refractive indices are chosen (Nilsson 1979) and are listed in table 1. The imaginary index of refraction is modelled assuming that most of the aerosol consists of weakly absorbing particles with $k < 10^{-4}$, mixed with a small number of highly absorbing particles with $k \sim 1.0$. Although Shettle and Fenn (1979) choose to represent mixtures of this type with a composite imaginary refractive index in the range $0.001 < k < 0.01$, which is close to the values obtained by various remote sensing and *in situ* techniques (Patterson and Grams 1984, Reagan *et al.* 1980), this procedure is not adopted here because as Bohren and Huffman (1983) point out, no common aerosol substance exists which has an imaginary index in this range. In the correction algorithm, the imaginary refractive index corresponding to the weakly absorbing particles is used. The imaginary refractive indices for the accumulation mode, which are listed in table 1, correspond to water while the values for the coarse particle mode correspond to crystalline quartz, which is constituent of atmospheric dust (Nilsson 1979). The aerosol refractive index is assumed to be constant with height.

The aerosol absorption in the model is the same as given by Shettle and Fenn (1979) for a rural aerosol with a relative humidity of 70 per cent. The absorption values $(1 - \omega_0)$ are given in table 1. The aerosol absorption optical thickness is given by $(1 - \omega_0)\tau_a$, where τ_a is the total aerosol thickness in the zenith direction. This value is added to the water vapour optical thickness ($\tau_w^{H_2O}$). The procedure is based on the assumption that the absorbing particles are small compared to the wavelength and that they occur separately from the other particles (external mode); in this case their scattering effects are small relative to their absorptive effects (Fraser and Kaufman 1985).

3.3. Altitude profiles

The radiative transfer computations depend on the altitude distributions of both the scattering and absorbing gases and aerosols. The atmospheric pressure profile used in the algorithm is adapted from the mid-latitude summer profile of McClatchey

Table 2. Aerosol size distribution parameters.

	Accumulation mode	Coarse particle mode
Geometric means radius r_n^i	0.0285	0.457
Standard deviation of the logarithm (base 10) of the radius σ_i	0.81	0.81
Number density N_i	0.999875	0.000125

et al. (1971). The altitude distribution of aerosols used in the algorithm is based on the 'average' distribution of Braslau and Dave (1973). The aerosol altitude distribution is first scaled to obtain the desired aerosol optical thickness.

Because the various gaseous absorbers described in the previous section have different altitude distributions, a composite altitude distribution is computed which accounts for all the absorbing gases including the aerosol absorption described in §3.2. In this method, the total gaseous absorption is divided into 'low' and 'high' components. The 'low' component consists of water vapour and aerosol absorption (τ_{gL}), while the 'high' component consists of ozone, oxygen, and CO₂ absorption (τ_{gH}). The 'low' component uses an altitude distribution based on the 'average' aerosol profile of Braslau and Dave (1973), while the 'high' component uses an altitude distribution based on the mid-latitude ozone profile of McClatchey *et al.* (1971).

3.4. Gaseous absorption

For the most part, the Landsat TM and NOAA AVHRR visible and near-infrared bands have been selected to minimize gaseous absorption. However, in some cases, the sensor channel is either relatively broad (as in the case of AVHRR band 2) or lies within a broad gaseous absorption band (as in the case of TM bands 2 and 3 which lie within the ozone continuum) so that the absorption by atmospheric gases can be both significant and variable. In the atmospheric correction algorithm, gaseous absorption was computed using the LOWTRAN 6 code (Kneizys *et al.* 1983) which computes atmospheric absorption from 0.250 μm to 28.5 μm . In the case of the AVHRR and TM bands, the absorbing gases are water vapour, carbon dioxide, oxygen, and ozone. The gaseous absorption optical thickness in the vertical direction due to gaseous species x for each band is computed using

$$\tau_g^x = -\ln \left[\frac{\int T_x L^m F_0 \psi d\lambda}{\int L^m F_0 \psi d\lambda} \right] \quad (11)$$

where T_x = transmittance due to gaseous species x . Since gaseous absorption is quite variable with time, the algorithm uses a weighted average of the absorption values computed using the tropical, mid-latitude summer, and mid-latitude winter atmospheres given in the LOWTRAN 6 code. The weighted average of the gaseous absorption τ_g^{x*} used in the algorithm is given by

$$\tau_g^{x*} = 0.25 \tau_{g1}^x + 0.5 \tau_{g2}^x + 0.25 \tau_{g3}^x \quad (12)$$

where τ_{g1}^x , τ_{g2}^x , and τ_{g3}^x are the gaseous absorption values computed using the mid-latitude winter, mid-latitude summer, and tropical values respectively. The absorption optical thicknesses due to water vapour, carbon dioxide, and ozone for each band are shown in table 1.

The algorithm can be applied to any specified gaseous optical thickness τ_g , however. An approximate correction is applied to L'_0 , F'_0 , s , and T in the lookup table to account for the excess (or deficit) in the absorption ($\Delta\tau_g$). The user may compute the required value of τ_g based on the sensor spectral response using the LOWTRAN program (Kneizys *et al.* 1983), for example. These corrections are discussed in the Appendix.

3.5. Molecular and aerosol optical thickness

The molecular scattering (or Rayleigh) optical thickness τ_{gs} is computed for sea level from (Hansen and Travis 1974)

$$\tau_{gs} = 0.008569 \lambda^{-4} (1 + 0.0113 \lambda^{-2} + 0.00013 \lambda^{-4}) \quad (13)$$

where the wavelength is in micrometres. This expression assumes the surface sea-level pressure is 1013 mb. In the case the surface is not at sea level, the value of the molecular scattering optical thickness τ_{gs} is assumed to vary according to:

$$\tau_{gs}(Z_0) = \tau_{gs}(0) \exp\left(\frac{-Z_0}{9}\right) \quad (14)$$

where Z_0 is the height of the surface above sea level in kilometres. In order to avoid a need for a new radiative transfer computation for each height of a surface, the computations are performed for $Z_0 = 0.4$ km, and the lookup table is adjusted each time the user specifies a different height. The algorithm adjusts the lookup table to account for the different molecular optical thickness by adjusting the wavelength of the radiation. Substitution of the relationship between λ and τ_{gs} (13 and 14) yields

$$\lambda(Z_0) = \lambda(0.4) \exp\left[\frac{(Z_0 - 0.4)}{36}\right] \quad (15)$$

For example, for $Z_0 = 0$ km, λ will decrease by 1.1 per cent, whereas for $Z_0 = 2$ km, λ will increase by 4.3 per cent. The combined aerosol and gaseous scattering phase function will have an error, but it will be small relative to the general uncertainty in the scattering phase function.

The relation between upward radiance and surface reflectance for each spectral band is computed for four aerosol optical thicknesses, $\tau_a = 0.0, 0.25, 0.50,$ and 1.00 , except for TM bands 5 and 7 where only the first two values are used. These values are selected to cover the range of aerosol optical thicknesses which could be expected for most remote sensing applications.

3.6. Measurement altitudes

The radiative transfer computations are tabulated at three measurement altitudes above the ground (not sea level): 0.45 km, 4.5 km, and 80 km. The algorithm will use these altitudes to interpolate to the input measurement altitude. Since 80.0 kilometres is above the atmosphere, corrections to satellite measurements are made with the 80 km tables.

3.7. Other algorithms

Two other algorithms have been developed for fast computations of radiation parameters. They do not calculate atmospheric corrections, however. Algorithm 5S developed by Tanré *et al.* (1986) calculates the radiance at satellite altitude for any wavelength of reflected sunlight. The LOWTRAN-7 algorithm developed by Kneizys *et al.* (1988) calculates the radiance and transmission at any altitude and wavelength greater than $0.2 \mu\text{m}$. The new algorithm introduced before this section can be applied to any height, but is restricted to wavelengths between 0.49 and $0.83 \mu\text{m}$ and 3 longer wavelengths. The present model is designed for a rural aerosol model. The 5S model includes in addition to the rural model, also maritime and urban models. The LOWTRAN-7 model also includes rural, maritime, and urban models.

4. Lookup tables

The lookup tables contain the radiation parameters, which have been computed previously and stored for use by the main program. Eight lookup tables are produced.

one table for each of the 2 AVHRR bands of 0.639 and 0.845 μm and one for each of the 6 TM bands of 0.486, 0.587, 0.663, 0.837, 1.663 and 2.189 μm . Each table is arranged for three heights of 0.45, 4.5 and 80.0 km above the ground. Each table contains values for nine solar zenith angles θ_0 (10, 20, 30, 40, 50, 60, 66, 72, and 78°), 13 observation zenith angles θ (0° to 78°, every 6°), 19 observation azimuth angles (0° to 180°, every 10°, plus 5° and 175°), and 4 aerosol optical thicknesses τ_a (0.0, 0.25, 0.50 and 1.0) for all wavelengths, except for 1.663 and 2.189 μm where only first two optical thicknesses of 0.0 and 0.25 are used.

5. Computational procedure

Input data to the correction program consists of the date for Earth–Sun distance correction, time for reference only, wavelength, aerosol and gaseous absorption optical thicknesses, solar zenith angle θ_0 , observation scan angle θ' , observation azimuth angle ϕ , height of the surface above sea level Z_0 , measurement height Z^m (equivalent to Z in 1), and the measured spectral radiance in absolute L^m or reflectance $L^{m'}$ units (option 1), or surface reflectance ρ (option 2). If the gaseous absorption optical thicknesses are not specified default values are used. The wavelength, solar and observation angles, and aerosol optical thickness data must be in the ranges discussed above as no extrapolation is performed. If the selected wavelength or altitude does not match the values used to construct the lookup table, the algorithm interpolates on wavelength and altitude as described above.

If option 1 is selected, the program computes the surface reflectance ρ , total spectral irradiance on the surface F_g , and total spectral radiance of the ground L_g in the direction of observation using (2), (4) and (5). The total spectral irradiance F_g is computed in $\text{Watts}/\text{m}^2/\mu\text{m}$ and total upward spectral radiance L_g is computed in $\text{Watts}/\text{m}^2/\mu\text{m}/\text{sr}$. If option 2 is selected, the program computes the absolute and normalized radiances L^m and $L^{m'}$, total spectral irradiance on surface F_g and the total upward spectral radiance L_g . If option 2 is selected, the only difference in the input parameters is to replace the measured radiance L^m by the surface reflectance ρ . Then the upward radiance is computed, rather than measured, for the height Z^m .

6. Errors

The errors in the surface reflectance derived from the measured radiances depend on many parameters: the model of the Earth–Atmosphere system, the algorithm, the accuracy of the variables that are specified, the viewing geometry, and the wavelength. Numerous sources of error in applying the correction algorithm are discussed by Fraser *et al.* (1989). We shall emphasize here the most important errors for correcting satellite measurements. The errors can be attributed to the model, the algorithm, and the input data.

6.1. Model

The surface is assumed to reflect light isotropically, whereas natural surface reflection is more or less anisotropic. Lee and Kaufman (1986) found that the error in derived surface reflectance of natural surfaces increased with the amount of haze and as the view direction approached the horizon. For light haze, the errors reach

$\Delta\rho = 0.02$ for the near-infrared and 0.01 for the visible spectra, except that the errors were larger in directions where the angular gradient of the reflectance was large.

The radiance of light scattered from models of the Earth-Atmosphere system is nearly linearly proportional to the surface reflectance (1), if that is the only varying independent variable, and if the optical thickness is less than 1. If the atmospheric parameters are perturbed, causing a perturbation of the simulated measured radiance, then the error in the surface reflectance derived from the simulated radiance is almost linearly proportional to the perturbation in the simulated reference.

The most important errors caused by the atmospheric model are due to aerosol absorption and the scattering phase function, when the aerosol optical thickness and gaseous absorptions are specified. Both terms on the right-hand-side of (1) have the same sign when the aerosol absorption is perturbed. For example, for representative remote sensing conditions ($\lambda = 0.55 \mu\text{m}$, $\tau_a = 0.29$, $\theta_0 = 0^\circ$, and $\theta = 60^\circ$) and a rather significant decrease in the albedo of single scattering of $\Delta\omega_0 = -0.20$, the surface reflectance error ranges from $\Delta\rho = -0.02$ to -0.11 as the reflectance increases from 0.0 to 0.6 .

When the aerosol scattering phase function for the backward hemisphere is changed, the two terms on the right-hand side of (1) have the opposite signs. The magnitude of the derived surface reflectance error diminishes with increasing surface reflectance. An estimate of the phase function error is obtained from ground-based measurements of the aerosol optical thickness and sky radiance. Kaufman (1990) has measured both the optical thickness and sky radiance at about 20 different sites on several continents (figure 1). These observations were made in rural and urban regions, which occasionally were affected by dust. The observations were made at seven wavelengths in the visible and near-infrared spectrum for a solar zenith angle of $\theta_0 = 60^\circ$. The sky radiance was measured at an azimuth 180° from the sun, or $\phi = 180^\circ$, and at a zenith angle of $\theta = 60^\circ$. For those observations when $\tau_a(0.522 \mu\text{m}) \leq 0.5$, the ratio of the standard error of estimate, given the aerosol optical thickness, to the mean sky radiance was 0.15 for the visible spectrum, but increased in the infrared spectrum to 0.32 for $\lambda = 0.872 \mu\text{m}$.

The sky radiance computed with the algorithm is biased low from the measured sky radiances in figure 1. This bias is less (greater) than the standard error of estimate for $\lambda = 0.522 \mu\text{m}$ ($0.872 \mu\text{m}$). Part of the bias is due to differences between the algorithm and actual values of aerosol albedo of single scattering and phase function. Part of the bias is due also to calibration of the radiometer. A conservative estimate of the errors caused by the phase function is given by an example where the phase function for scattering in the backward hemisphere increases by 40 per cent ($\lambda = 0.55 \mu\text{m}$, $\tau_a = 0.25$, $\theta_0 = 0^\circ$, and $\theta = 60^\circ$). Then the surface reflectance error decreases linearly from 0.038 to 0.003 as the surface reflectance increases from 0.0 to 0.6 .

Additional algorithm errors result from neglect of the polarization characteristics of the radiation when computing the radiation parameters in the lookup tables. The polarization errors are caused by the polarized light resulting from multiple scattering within the atmosphere, if radiation reflected from the surface is weak or weakly polarized. The intensity of multiple scattering increases with decreasing wavelength. If polarization is neglected, simulation studies, show that the error in derived surface reflectance increases from less than 3 per cent for $\lambda \geq 639 \text{ nm}$ to 10 per cent for $\lambda = 486 \text{ nm}$.

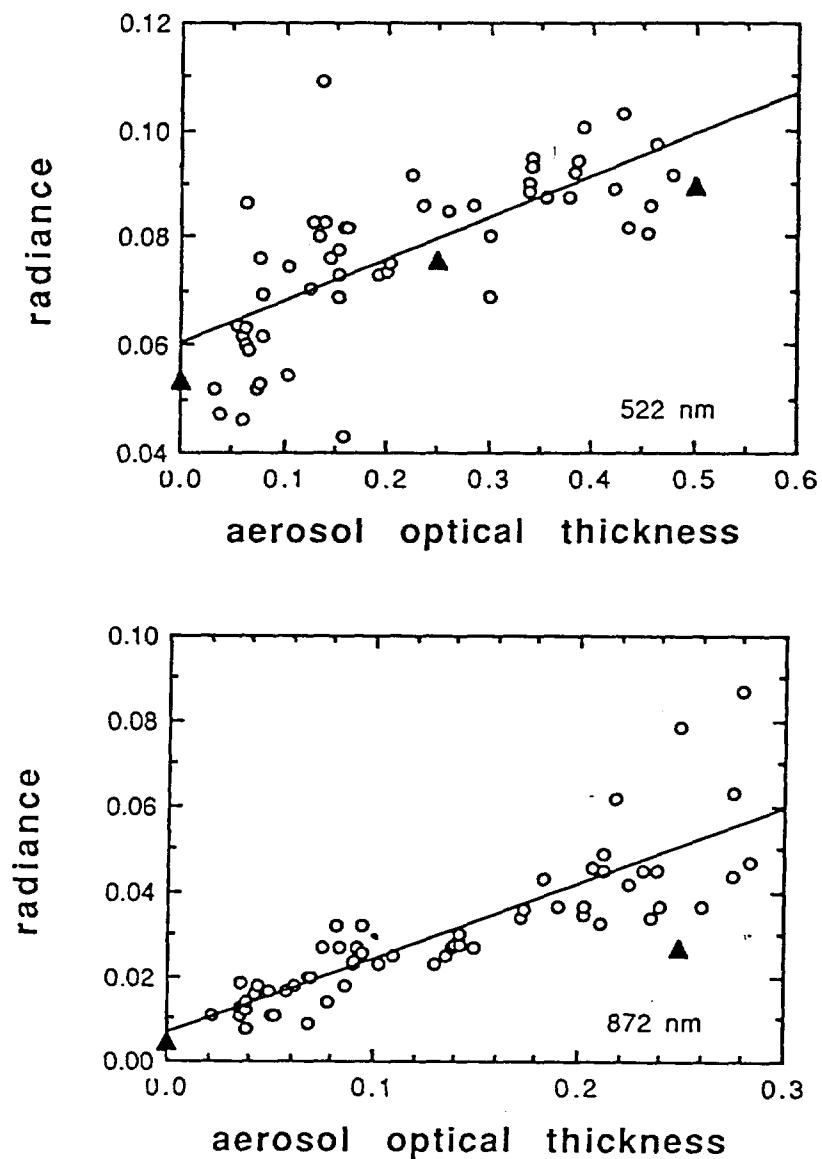


Figure 1. Measured radiance of skylight at the ground ($\theta_o = \theta = 60^\circ$, $\phi = 180^\circ$) as a function of aerosol optical thickness. The radiance $= (\pi L^m / F_o)$. The triangles show values computed for a rural atmosphere. Data are given by Kaufman (1990).

The vertical distribution of aerosols is not important when the solar zenith and view angles are not large, and the aerosol optical thickness is not large, if the aerosol lies below the viewing platform. If an aircraft is within the aerosol layer, then the distribution may account for appreciable errors in the derived reflectances.

6.2. Interpolation errors

The tabulated parameters L'_o , F'_d , and T/π are interpolated linearly for the observing height Z and directions θ_o , θ , and ϕ . The exponential values of L'_o , F'_d , s ,

and T/π are interpolated linearly with respect to optical thickness, however. The derived reflectance errors caused by interpolations in the lookup tables are less than 10 per cent, when the surface reflectance $\rho=0.05$, if the solar zenith and nadir observation angles are not large. The errors become larger if both the solar zenith and nadir measurement angles become large ($\theta_0=74^\circ$ and $\theta=56^\circ$). When the surface reflectance $\rho=0.05$, for example, the surface reflectance error is as large as $|\Delta\rho/\rho|=0.32$ when measuring 15° in azimuth from the sun but reduces to 0.08 when measuring backward reflectance.

6.3. Input errors

Since the measured radiance is nearly a linear function of the surface reflectance, if that is the only independent variable, the ratio of errors in the surface reflectance and the radiance is almost constant. If the radiance error is a constant percentage of the radiance, however, the reflectance error increases with reflectance. Surface reflectance errors that can be expected for a 10 per cent radiance error and representative measurement conditions ($\lambda=0.61\ \mu\text{m}$, $\tau_a=0.25$, $\omega_0=0.96$, $\theta_0=40^\circ$, $\theta=60^\circ$, $\phi=0^\circ$) increase in absolute value from 0.01 to 0.05 as the surface reflectance increases from 0.0 to 0.4.

The derived surface reflectance is in error, if the actual and model aerosol optical thicknesses are not the same. An optical thickness error, say positive, results in an overestimation of the path radiance but an underestimation of transmission (1). The transmission effect increases with increasing reflectance, and the two terms on the right-hand side tend to compensate. An optical thickness error usually causes the largest reflectance errors, when the surface reflectance is weak. For an optical thickness error of $\Delta\tau_a=0.1$ and the same conditions given in the previous paragraph, except that there is no error in the measured radiance, the reflectance error decreases from 0.03 to 0.01 as the reflectance increases from 0.0 to 0.4.

Another source of error is caused by using an incorrect value of the gaseous absorption. Most of the gaseous absorption in the Landsat TM and NOAA AVHRR visible and near IR bands is contributed by either water vapour or ozone. For water vapour this occurs for AVHRR band 2 while for ozone this occurs for TM band 2.

Since the amount of an absorbing gas is variable, the algorithm uses a weighted average of the gaseous absorption transmissions. Most of the weight is given to the mid-latitude summer profile. In the case of AVHRR band 2, the algorithm uses a water vapour gaseous absorption optical thickness of $\tau_g=0.0933$, which is the default value. If the default value is used when the mid-latitude winter value of $\tau_g=0.0486$ occurs, the derived surface reflectance error is 0.02 for a surface reflectance is 0.20 and typical remote sensing parameters.

The default value of ozone absorption optical thickness is $\tau_g=0.032$ for TM band 2. If the default value is used instead of the mid-latitude winter ozone absorption optical thickness $\tau_g=0.039$ or the tropical value of $\tau_g=0.024$, the magnitude of errors in the derived surface reflectance is 0.002 when the surface reflectance is 0.05.

The derived surface reflectance errors are small for errors in the geometrical parameters. For errors of $\Delta\theta_0=\Delta\theta=\Delta\phi=2^\circ$ the surface reflectance errors are generally less than 2 per cent of the surface reflectance.

7. Conclusion

An algorithm is developed to account for atmospheric effects when deriving surface reflectance properties from visible and near-infrared radiances measured by

aircraft or satellite over rural areas. The radiance that would be measured for a given surface reflectance can be derived, also. The algorithm uses a tabulated set of radiation parameters that are computed for various wavelengths, solar and observation angles, and aerosol optical thicknesses. All aerosol parameters have been assumed, except for the aerosol optical thickness, which is an input value. Since the algorithm performs essentially interpolations, it is fast; therefore, it is well suited for reducing observations in many wavelengths.

A complete error analysis in the derived surface reflectance from remote measurements of radiance is not given because of a wide range in remote sensing conditions involving measurements and atmospheric states. If the aerosol and water vapour optical thicknesses are specified with reasonable accuracy, the largest errors result from the fixed values of absorption and scattering phase function for the aerosol model. The algorithm values apply to a rural aerosol model. If the actual and model aerosol values have large differences, the error in the derived surface reflectance can be large. However, the algorithm could be easily modified for use with other aerosol properties by replacing the lookup tables with radiation parameters generated for the more appropriate aerosol.

Appendix

The correction algorithm accepts as input the gaseous absorption optical thicknesses τ_{gL} and τ_{gH} . They usually differ from the default values by a small amount $\Delta\tau_{gL}$ and $\Delta\tau_{gH}$. The method of accounting for the gaseous absorption in satellite measurements is presented. The method for aircraft measurement corrections is similar and not discussed. The perturbed values of transmission and irradiance at the ground are

$$T(\mu) + \Delta T(\mu) = T(\mu) \exp(-(\Delta\tau_{gL} + \Delta\tau_{gH})/\mu) \quad (\text{A } 1)$$

$$F_d + \Delta F_d = F_d \exp(-(\Delta\tau_{gL} + \Delta\tau_{gH})/\mu_0) \quad (\text{A } 2)$$

T and F_d are the default values of the transmission and irradiance. The values on the left-hand side of the equations are used for the atmospheric corrections.

The adjustments for the atmospheric reflectance s and path radiance L_0 are based on the assumption that the molecular scattering layer, which is designated by the subscript H, lies above a thin boundary layer containing the aerosol, which is designated by the subscript L. Ozone and water vapour are the most important variable, absorbing gases. The ozone is assumed to lie above the upper, scattering layer. The water vapour is assumed to occupy the lower, aerosol layer.

We assume that the reflectance s is given by the following equation:

$$s = \frac{F_L + F_H}{F} \quad (\text{A } 3)$$

where F_L and F_H are downward fluxes at the ground scattered by the lower and higher layers, respectively, and F is the upward flux at the ground. Since the reflectance of the lower layer is given by the equation

$$s_L = F_L/F \quad (\text{A } 4)$$

the perturbed reflectance is given by

$$s_L + \Delta s_L = \frac{F_L + \Delta F_L}{F} \quad (\text{A } 5)$$

Assume that the energy is reflected from the middle of the lower layer. Then

$$F_L + \Delta F_L = F_L \exp \left[-\frac{\Delta\tau_{gL}}{2} \left(\frac{1}{\mu'} + \frac{1}{\mu''} \right) \right] \quad (\text{A } 6)$$

where μ' and μ'' are effective cosines for transmission of flux and are usually assumed for $\mu' = \mu'' = 0.5$. Substitution of (A 6) in (A 5) yields

$$s_L + \Delta s_L = s_L \exp(-2\Delta\tau_{gL}). \quad (\text{A } 7)$$

The reflectance of the upper layer is similar, except that the downward flux from it is reduced by the two-way transmission through the lower layer:

$$s_H + \Delta s_H = s_H \exp(-4\Delta\tau_{gL}). \quad (\text{A } 8)$$

s_H is not affected by the absorbing gas above the upper layer. Substitution of (A 7) and (A 8) in (A 3) yields the total reflectance

$$s + \Delta s = s \exp(-2\Delta\tau_{gL}) \left\{ 1 - \frac{s_H}{s} \exp(-2\Delta\tau_{gL}) [1 - \exp(-2\Delta\tau_{gL})] \right\} \quad (\text{A } 9)$$

The second-order correction term, with s_H/s as a coefficient, is neglected. Its maximum contribution occurs for the AVHRR band at 845 nm. When the aerosol optical thickness is zero, ($s_H/s = 1$) and taking a maximum value of $\Delta\tau_{gL} = 0.1$, the second-order correction is less than 0.2. However, $s = 0.01$, and it is changed by only 0.002. As the aerosol optical thickness increases to 1, s increases to 0.16, the second-order correction decreases to 0.06, and the second-order correction contributes 0.004 to s . Hence the corrected reflectance is

$$s + \Delta s = s \exp(-2\Delta\tau_{gL}). \quad (\text{A } 10)$$

We assume that the normalized path radiance equals the sum of the radiances from the lower layer (L'_{oL}) and the higher layer (L'_{oH}):

$$L'_o = L'_{oL} + L'_{oH} \quad (\text{A } 11)$$

If we assume that the path radiance from the lowest layer originates at the middle of that layer, then

$$L'_{oL} + \Delta L'_{oL} = L'_{oL} \exp \left[-A \left(\frac{\Delta\tau_{gL}}{2} + \Delta\tau_{gH} \right) \right]. \quad (\text{A } 12)$$

The corrected radiance of the upper layer is

$$L'_{oH} + \Delta L'_{oH} = L'_{oH} \exp(-A\Delta\tau_{gH}), \quad (\text{A } 13)$$

$$A = \frac{1}{\mu} + \frac{1}{\mu_o}. \quad (\text{A } 14)$$

The corrected path radiance is obtained by substituting (A 12) and (A 13) in (A 11):

$$L'_o + \Delta L'_o = L'_o \exp \left[-A \left(\frac{\Delta\tau_{gL}}{2} + \Delta\tau_{gH} \right) \right] + \left[1 + \frac{L'_{oH}}{L'_o} \exp \left[\left(\frac{A}{2} \Delta\tau_{gL} \right) - 1 \right] \right] \quad (\text{A } 15)$$

The second-order term on the right-hand side, where the coefficient is L'_{oH}/L'_o , makes the largest contribution for AVHRR channel 2 at 845 nm. For extreme conditions of large amount of haze and large slant paths through the atmosphere ($\theta_0 = 60^\circ$, $\phi = 0^\circ$,

and $\tau_a = 1.0$), the error in the derived surface reflectance is only 0.01. Otherwise the derived surface reflectance error due to this term is less. Hence this term is neglected. The corrected path radiance for gaseous absorption is

$$L'_0 + \Delta L'_0 = L'_0 \exp \left[-A \left(\frac{\Delta\tau_{gL}}{2} + \Delta\tau_{gH} \right) \right]. \quad (\text{A } 16)$$

References

- BOHREN, C. F., and HUFFMAN, D. R., 1983, *Absorption and Scattering of Light by Small Particles* (New York: John Wiley).
- BRASLAW, N., and DAVE, J. V., 1973, Effect of aerosols on the transfer of solar energy through realistic model atmospheres. Part I: Non-absorbing aerosols. *Journal of Applied Meteorology*, **12**, 601–615.
- CHANDRASEKHAR, S., 1950, *Radiative Transfer* (London: Oxford University Press).
- DAVE, J. V., 1972a. Development of programs for computing characteristics of ultraviolet radiation. Technical Report, Scalar Case, Program I, FSC-72-0009, IBM Federal Systems Division, Gaithersburg, Maryland.
- DAVE, J. V., 1972b. Development of programs for computing characteristics of ultraviolet radiation. Technical Report, Scalar Case, Program II, FSC-72-0011, IBM Federal Systems Division, Gaithersburg, Maryland.
- DAVE, J. V., 1972c. Development of programs for computing characteristics of ultraviolet radiation. Technical Report, Scalar Case, Program III, FSC-72-0012, IBM Federal Systems Division, Gaithersburg, Maryland.
- DAVE, J. V., 1972d. Development of programs for computing characteristics of ultraviolet radiation. Technical Report, Scalar Case, Program IV, FSC-72-0013, IBM Federal Systems Division, Gaithersburg, Maryland.
- FERRARE, R. A., FRASER, R. S., and KAUFMAN, Y. J., 1990, Satellite remote sensing of large scale air pollution—measurements of forest fires smoke. *Journal of Geophysical Research*, **95**, 9911–9925.
- FRASER, R. S., and KAUFMAN, Y. J., 1985, The relative importance of aerosol scattering and absorption in remote sensing. *IEEE Transactions on Geoscience and Remote Sensing*, **23**, 625–633.
- FRASER, R. S., FERRARE, R. A., KAUFMAN, Y. J., and MATTOO, S., 1989, Algorithm for Atmospheric Corrections of Aircraft and Satellite Imagery, NASA TM-100751, 98 pp. This document can be obtained by giving: Accession No. N9013976 and ordering from: National Technical Information Service, 5285 Port Royal Road, Springfield, VA 22161, Telephone number: 703-487-4650).
- HANSEN, J. E., and TRAVIS, L. D., 1974, Light scattering in planetary atmospheres. *Space Science Reviews*, **16**, 527–610.
- KAUFMAN, Y. J., 1991, Measurements of the aerosol optical thickness and the path radiance—implication on aerosol remote sensing and atmospheric corrections. *IEEE Transactions on Geoscience and Remote Sensing*, in press.
- KAUFMAN, Y. J., and SENDRA, C., 1988, Automatic atmospheric correction. *International Journal of Remote Sensing*, **9**, 1357–1381.
- KAUFMAN, Y. J., FRASER, R. S., and FERRARE, R. A., 1990, Satellite remote sensing of large scale air pollution—method. *Journal of Geophysical Research*, **95**, 9895–9909.
- KIDWELL, C. D., 1985, NOAA Polar Orbiter Data User's Guide, NOAA-NESDIS Washington, D.C., 20233.
- KNEIZYS, F. X., SHETTLE, E. P., GALLERY, W. O., CHETWYND, J. H., ABREU, L. W., SELBY, J. E. A., CLOUGH, S. A., and FENN, R. W., 1983, Atmospheric transmittance radiance: computer code LOWTRAN 6. AFGL-TR-83-0187 Air Force Geophysics Laboratory Hanscom AFB, Massachusetts.
- KNEIZYS, F. X., SHETTLE, E. P., ABREU, L. W., CHETWYND, J. H., ANDERSON, G. P., GALLERY, W. O., SELBY, J. E. A., and CLOUGH, S. A., 1988, Users guide to LOWTRAN 7. AFGL-TR-88-0177, Air Force Geophysics Laboratory Hanscom AFB, Massachusetts.

- LEE, T. Y., and KAUFMAN, Y. J., 1986, The effects of surface non-Lambertianity on remote sensing of ground reflectance and vegetation index. *IEEE Transactions on Geoscience and Remote Sensing*, **24**, 698-708.
- MARKHAM, B., and BARKER, J. L., 1985, Spectral characterization of the Landsat TM sensors. *Landsat-4 Science Characterization—Early Results*, **2**, Goddard Space Flight Center, Greenbelt, MD, 20771, NASA Conference Publications 2355, 235-276.
- MCCLATCHY, R. A., FENN, R. W., SELBY, J. E. A., VOLZ, F. E., and GARING, J. S., 1971, Optical properties of the atmosphere. AFCRL-71-0279. Air Force Cambridge Research Laboratory, Hanscomb AFB, Massachusetts.
- NECKEL, H., and LAMBS, D., 1984, The solar radiation between 3300 and 12500 Å. *Solar Physics*, **90**, 205-258.
- NILSSON, B., 1979, Meteorological influence on aerosol extinction in the 0.2-40 μm wavelength range. *Applied Optics*, **18**, 3457-3473.
- PATTERSON, E. M., and GRAMS, G. W., 1984, Determination of aerosol absorption and scattering in the free troposphere. *IRS '84: Current Problems in Atmospheric Radiation, Proceedings of the International Radiation Symposium, Perugia, Italy, 21-28 August 1984* (Hampton, Virginia: Deepak) pp. 29-31.
- REAGAN, J. A., BYRNE, D. M., KING, M. D., SPINHIRNE, J. D., and HERMAN, B. M., 1980, Determination of the complex refractive index of atmospheric particulates from bistatic-monostatic lidar and solar radiometer measurements. *Journal of Geophysical Research*, **85**, 1591-1599.
- SELLERS, P. J., HALL, F. G., ASRAR, G., STREBEL, D. E., and MURPHY, R. E., 1988, The First ISLSCP Field Experiment (FIFE). *Bulletin of the American Meteorological Society*, **69**, 22-27.
- SHETTLE, E. P., and FENN, R. W., 1979, Models for the aerosols of the lower atmosphere and the effects of humidity variations on their optical properties. AFGL-TR-79-0214. Air Force Geophysics Laboratory, Hanscom AFB, Massachusetts.
- TANRÉ, D., DEROO, C., DUHAUT, P., HERMAN, M., MORCRETTE, J. J., PERBOS, J., and DESCHAMPS, P. Y., 1986, Simulation of the satellite signal in the solar spectrum (5S). Laboratoire d'Optique Atmosphérique, Université des Sciences et Techniques de Lille, 59655 Villeneuve d'Ascq Cédex, France.